

# EFFECT OF HEAT TREATMENT ON THE HARDNESS AND ABRASIVENESS OF ALMANDINE AND PYROPE GARNET FOR WATER-CUTTING OF MARBLE

Mahmoud A. Rabah

Chemical and electrochemical laboratory, Mineral Processing Dept.

Central Metallurgical Research and Development Institute (CMRDI).

P.O.Box 87 Helena 11421 Cairo Egypt.

[Mrabah010@gmail.com](mailto:Mrabah010@gmail.com)

[mahmoud.rabah@ymail.com](mailto:mahmoud.rabah@ymail.com)

+2 27142454 +2 27142451 Mobile +2 01006608672

**Abstract**— Garnet has been used for decades as an abrasive in water jet cutting and sand blasting because of its superior physical properties. When added to use in water-cutting process of marble. A standard commercial sample of the mineral was tested in terms of the hardness and abrasiveness properties. The sample was sized to 4 fractions having the size of < 60 um, >60<100 um, >100<180 um >1280<250 and 250 um designated the symbols, FF, MF, MC and C respectively. Each sample was separately heated in controlled conditions at temperatures up to 1000°C at a heating rate of 10°C/min in an electrically heated chamber furnace. Soaking time at the maximum temperature was up to 6 h. Hardness and abrasiveness properties of the heat treated samples were tested to cut marble having a thickness of 25 mm. Results revealed that H/A of the natural garnet mineral increased by heating at temperatures up to 600°C and exhibited pronounced decrease with higher temperatures up to 1000°C. Results were explained in the light of a structural irreversible dislocation (SD) of the crystals of garnet almandine  $\text{Fe}_2^{+3}\text{Al}_2\text{Si}_3\text{O}_{12}$  and pyrope  $\text{Mg}_3\text{Al}_2\text{Si}_3\text{O}_{12}$ . Characterization of the mineral was carried out with the help of XRD, SEM and FT-IR measurements.

**Index Terms**— Garnet abrasive, heat treatment, water jet cutting, hardness abrasiveness.

## I. INTRODUCTION

The electronic structure and bonding of  $\text{Gd}_3\text{Sc}_2\text{Ga}_3\text{O}_{12}$ (GSGG),  $\text{Gd}_3\text{Sc}_2\text{Al}_3\text{O}_{12}$ (GSAG), and  $\text{Gd}_3\text{Ga}_5\text{O}_12$ (GGG) crystals with a garnet structure high pressure streams of water, garnet abrasive is capable of cutting through tough materials including steel, aluminum, stone, and Inconel. This study shows the effect of heat treatment of low size particles of natural garnet mineral on its hardness and abrasiveness (H/A) [1]. Results were compared with a similar calculation on yttrium aluminum garnet [Y<sub>3</sub>Al<sub>5</sub>O<sub>12</sub>(YAG)].The calculated equilibrium volumes of the three crystals are close to the measured volumes with a slight overestimation for GGG. GGG also has a smaller bulk modulus than the other three crystals. The calculated density of states and their atomic and orbital

decompositions are presented and contrasted. All four crystals show very similar band structures and inter atomic bonding. However, it is found that in GSGG and GSAG crystals, the Sc atom at the octahedral site shows a higher covalent character and an increased bond order in comparison to Ga or Al at the same site. This result may provide some insight into the significant difference in the radiation hardness of  $\text{Cr}^{3+}$   $\text{Nd}^{3+}$

:GSGG as compared to  $\text{Nd}^{3+}$  :YAG. Some garnet collected from Khammam district, Andhra Pradesh India were characterized [2]. Garnets were found to have cubic symmetry with no cleavage. Present garnets are of pink color with reasonably large dimensions.

Mao et al. [3] measured synchrotron Mossbauer spectra (SMS) of the high-spin Fe<sup>2+</sup> in Fe bearing pyrope garnet with two distinct compositions,  $(\text{Mg}_0.8\text{Fe}_0.2)_3\text{Al}_2\text{Si}_3(\text{py}_80\text{alm}_20)$ and  $\text{Fe}_3\text{Al}_2\text{Si}_3\text{O}$  (alm100), up to 30 GPa and 750 K. Analyses of the SMS spectra revealed that the high-spin Fe<sup>2+12</sup> ions in the distorted dodecahedral site exhibit extremely high QS of ~3.4–3.6 mm/sand relatively high chemical shifts (CS) of ~1.2–1.3 mm/s at high *P-T*, indicating that the Fe ions remain in the high-spin state. An increase in the Fe content in the pyrope-almandine series only slightly decreases the QS and CS of the Fe ions. To decipher the energy separation ( $\Delta$ ) between the two lowest energy levels of the 3d electrons of the Fe<sup>2+2+</sup> ions in the sample, the *dxy* and *d* orbitals, and the QS values of py80alm20 at high *P-T* were further evaluated using Huggins model. Our modeled results show that the  $\Delta$  of the Fe ions in py80alm20 is ~156 meV at high *P-T*, and may be correlated to the change of the crystal-field energy splitting ( $\Delta_2+C$ ). Comparison of the QS,  $\Delta$ , and  $\Delta$  ions in the distorted dodecahedral sites of pyrope and silicate perovskite indicates that the high-spin FeC with the extremely high QS can remain stable at high *P-T* conditions, consistent with recent theoretical predictions. Our results thus contribute to our current understanding of the hyperfine parameters and spin and valence states of iron in the mantle silicate minerals at high *P-T*. Considering the similarity in the crystallographic environments and the magnitude of the QS of Fe on Fe-

bearing pyrope, perovskite, and post-perovskite, experimental studies [2] on the local electronic structures and hyperfine parameters of Fe-bearing pyrope as a function of  $P-T$  can provide new insights into the spin states of Fe in the lower-mantle minerals. The QS and chemical shift (CS) of Fe-bearing pyrope have only been determined by Mössbauer spectroscopy at temperatures up to 800 K under ambient pressure in previous studies (Huggins 1975 [4], Amthauer et al. 1976 [5]; Murad and Wagner 1987 [6]; Geiger et al. 1992 [7]; Cerná et al. 2000 [8]). The combined effects of  $P-T$  on these parameters remained require studies, significantly limiting the electronic structures of Fe-bearing pyrope and other major rock-forming silicates at high  $P-T$ . In this study, we have measured and analyzed SMS spectra of two Fe-bearing pyropes at  $P-T$  conditions relevant to the Earth's upper mantle. K. Barcova, et al., [9] reported that the thermal decomposition of almandine garnet from Zoltye Vody, Ukraine, has been studied using  $^{57}\text{Fe}$  Mössbauer spectroscopy. Room temperature Mössbauer spectrum of the initial powdered sample is characterized by one doublet corresponding to  $\text{Fe}^{2+}$  in dodecahedral position 24c. In the room temperature spectra of all heated almandine samples, a doublet corresponding to  $\gamma\text{-Fe}_2\text{O}_3$  nanoparticles appeared. Depending on experimental conditions (heating temperature and time), the additional spectral lines of  $\alpha\text{-Fe}_2\text{O}_3$  and  $\varepsilon\text{-Fe}_2\text{O}_3$  were observed in Mössbauer spectra.

Zboril et al. [10] showed that pyrope-type garnet with a dominant magnesium content at position 24c in the cubic garnet structure undergo oxidative decomposition at 1200°C resulting in the formation of the paramagnetic spinel  $\text{Mg}(\text{Al},\text{Fe})_2\text{O}_4$  structure with a low iron content, enstatite  $(\text{Mg},\text{Fe})\text{SiO}_3$  and anorthite  $\text{CaAl}_2\text{Si}_2\text{O}_8$  as the host compound for calcium. Contrary to pyropes, the iron-rich garnets exhibit complete oxidation at 1200°C conforming to the formation of magnetically ordered nanocrystalline  $\gamma\text{-Fe}_2\text{O}_3$  or  $\text{Mg}(\text{Fe},\text{Al})_2\text{O}_4$  spinels depending on the initial chemical composition of the garnets. In the reaction products of iron-rich garnets, cordierite ( $\text{Mg}_2\text{Al}_3\text{Si}_5\text{O}_{18}$ ) and anorthite were identified as non-ferrous phases. Zboril et al [11] reported that At 1000 °C, the non-destructive oxidation of  $\text{Fe}^{2+}$  in air includes the partial stabilization of  $\text{Fe}^{3+}$  in the dodecahedral 24c position of the garnet structure and the simultaneous formation of hematite particles (15–20 nm). The incorporation of the magnesium ions to the hematite structure results in the suppression of the Morin transition temperature to below 20 K. The general garnet structure is preserved during the redox process at 1000 °C, in accordance with XRD and DTA data. At 1100 °C, however, oxidative conversion of pyrope to the mixed magnesium aluminium iron oxide, Fe-ortho-enstatite and cristobalite was observed. During this destructive decomposition,  $\text{Fe}^{2+}$  is predominantly oxidized and incorporated into the spinel structure of  $\text{Mg}(\text{Al},\text{Fe})_2\text{O}_4$  and partially stabilized in the structure of orthoenstatite,  $(\text{Mg},\text{Fe})\text{SiO}_3$ . The combination of XRD and Mössbauer data suggest the definite reaction mechanism prevailing, including the refinement of the chemical composition and quantification of the reaction products. The reaction mechanism indicates that the respective distribution of  $\text{Fe}^{2+}$  and  $\text{Fe}^{3+}$  to the enstatite and spinel structures is determined by the total content of  $\text{Fe}^{2+}$  in pyrope. O. Schneeweiss et al., [12] showed that it was obvious that the thermal transformation of almandine garnet in air is related to

the primary formation of  $\gamma\text{-Fe}_2\text{O}_3$  super paramagnetic nanoparticles.  $\gamma\text{-Fe}_2\text{O}_3$  nanoparticles are transformed into  $\varepsilon\text{-Fe}_2\text{O}_3$  and consequently into  $\alpha\text{-Fe}_2\text{O}_3$  at higher temperatures. The mechanism and kinetics of the individual structural transformations depend on experimental conditions — mainly on the heating temperature and size of the particles.

The objectives of this work are to explore the effect of heating almandine and pyrope garnet in ambient pressure at temperatures up to 1000°C for different periods on the abrasiveness and hardness properties for water jet cutting of marble. Different parameters of heating rate (10, 20 and 30°C/min) and soaking time at the maximum temperature (10,15 and 20 minutes) were considered,

## II. EXPERIMENTAL

### A Materials and Methods

- a- Garnet samples were mined from the Ras Abu Rudeis, and El Tor places at the eastern and south offshore of Sinai, Egypt. About 50 kg of the mineral was mined manually. The sample was visually examined whereby foreign contaminants were rejected. It was then washed with hot water and dried at 105°C in a drying oven for about 6 h. About 1 kg was crushed in a double roller mill and sieved to pass mesh sizes as follows: >60<100 um, >100<180, >180<240 and 250 um designated the symbols, FF, MF, MC and C respectively.
- b- The samples were heated in a chamber furnace type Nedertherm (Netherland) fitted with C30 controller. Heating regime was adjusted at a an increasing rate of 10°C/min. Soaking at the maximum temperature was kept constant at 3h.

### B - Measurement of physical properties

a- ensity was measured using Density Ultrapyc 1200e gas pycnometer of Quantachrome Instruments, Florida USA and density bottle method

b- Hardness was measured as Rockwell hardness using hardness tester model DHT-100 NDT Vendor, Denmark.

c- Abrasiveness of the garnet samples was measured applying the technique reported by Abdel Aal 2006 [13].

#### d- Particle size determination

Particle size was determined using particle size analyzer type. The machine was fitted with a set of standard sieves – 400 +10 um.

e- Workability of the garnet particles. The length of cut marble having smooth surface was measured. Cutting was carried out using an industrial bridge cutting machine type WC5WA2013H, California USA. The water was loaded with 10% of garnet particles. Cutting was displayed at constant flow rate, pressure of 420 Mpa max. Marble sample was 10 mm in thickness. Fig.1a, 1b show the cutting facility [14].

- f- Bi-distilled water was used for analysis and physical measurements. The Density of water was taken as 0.978 g/cm<sup>3</sup>.

### loss of the garnet particles



**Fig.1a**

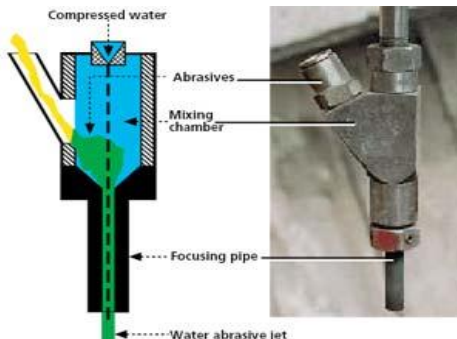
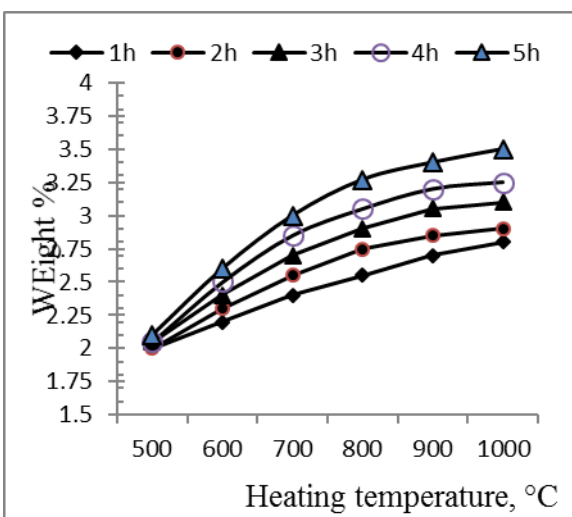


**Fig. 1b The cutting facility [14]**

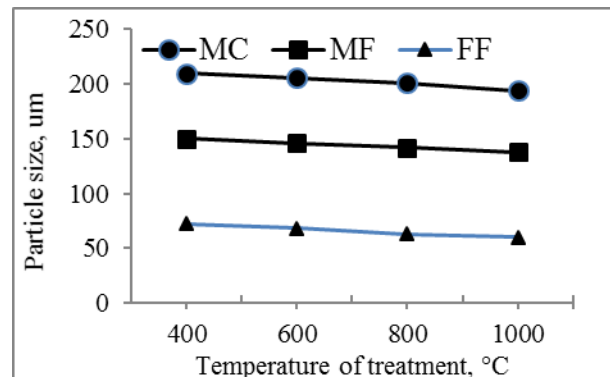
### III. RESULTS

Figure 2 shows the weight change as a function of thermal treatment of the mineral in open atmosphere. It can be seen that the weight loss exhibits slight and gradual increase with rise in temperature up to 1000°C. It is also seen that the magnitude of weight loss increases with increase in heating time up to 5 h.

Fig 3 shows the effect of treatment temperature on the particle size of the garnet mineral. It is seen that particle size of the grains decreases with the increase in temperature of treatment. The slope of the extent of decrease is nearly the same irrespective of the particle size of the raw garnet mineral

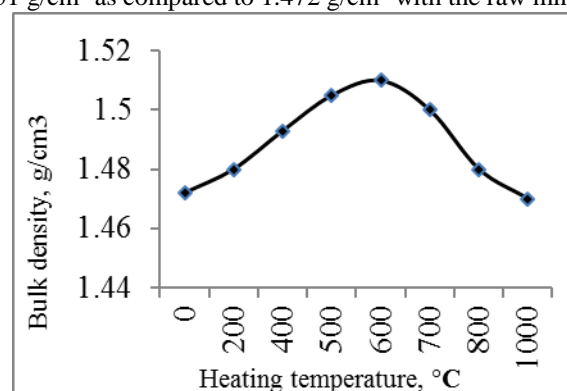


**Fig. 2 Effect of heating garnet mineral on the weight**



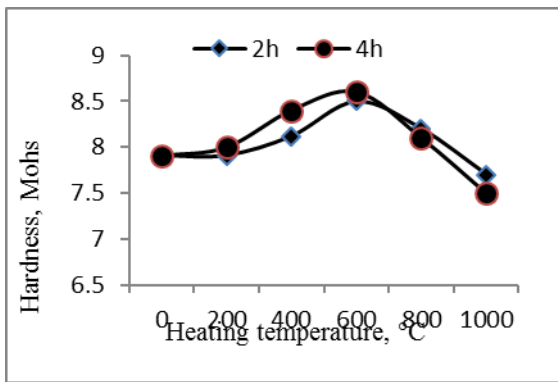
**Fig. 3 Effect of heating temperature on the particle size of garnet mineral**

Figure 4 shows the bulk density value of MF garnet particles as affected by heating at temperatures up to 1000°C for 5 hours. It can be seen that the bulk density value increases with increase in temperature passing through a maximum at 600°C. The bulk density value at the maximum amounts to 1.51 g/cm³ as compared to 1.472 g/cm³ with the raw mineral



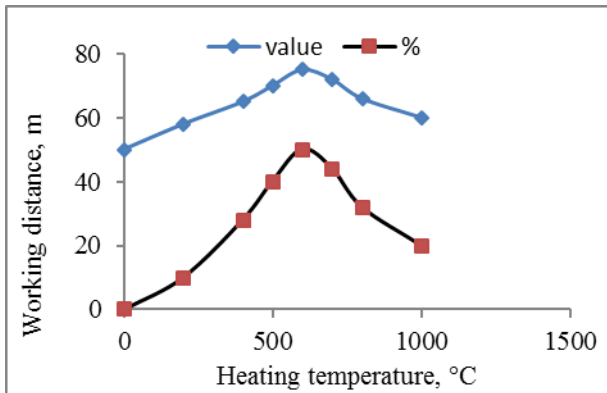
**Fig. 4 Effect of heating the MF garnet particles on bulk density value**

Figure 5 illustrates the hardness in Mohs of the garnet samples as affected by heat treatment. It can be seen that the hardness of the garnet mineral increases with increase in heating temperature up to 600°C whereby the optimum value of hardness has attained. With further increase in temperature, the hardness value gradually decreases. It is also seen the effect of time of heating has only a minor significant effect. Heating up to 600°C for 4 hours displays higher hardness magnitude as compared to the hardness after heating at the same temperature for 2 hours



**Fig.5 Hardness in Mohs as a function of heat treatment of garnet MF particles**

Fig. 6 shows the effect of heating the garnet particles on the cutting distance of marble 10 mm in thickness using a water jet load with 10 % of garnet particles. It can be seen that the length of the cut marble increases from 50 m to 80 m corresponding to 60% increase.



**Fig. 6 Effect of heating the garnet particles on the workability of the garnet particles.**

#### I- Discussion

Garnet is a mineral having the chemical structure [15]: It is built up from Schematic O-atom coordination polyhedral in the

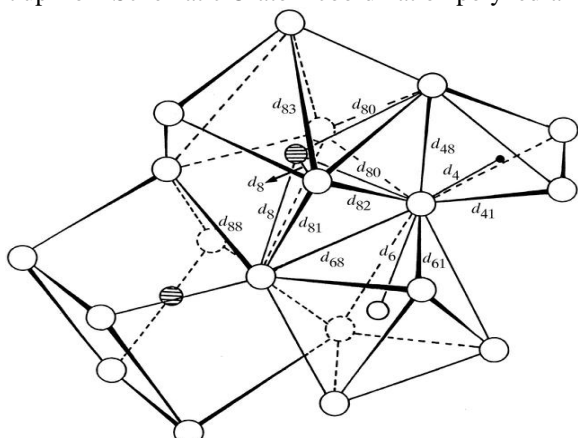


**Fig. 7 The octahedral structure of garnet [15]**

garnet structure (Novak & Gibbs, 1971 ). Large open circles, hatched circles, small open circles and small filled

circles represent O atoms, the dodecahedral-site cations [16], The octahedral structure is shown in Fig. 7.

The authors reported that oxygen bonded to one Ca and one Mg, indicating that there are two distinct bond distances for the Mg-O and/or Ca-O bonds through the entire solid solution. Heating of the mineral at 600°C increases the density by about 0.28 %. Density change can be ascribed to structural changes. The later phenomenon involves oxidation of some iron and magnesium atoms to a higher state of oxidation with subsequent decrease of the bond distance for Fe-O and for Mg-O i.e. partial collapse of the garnet crystals. It is worthy to note that density value decreases with further increase in heating temperature up to 1000°C. The mineral view is given in Figs 8a through 8d.

Analysis of the garnet samples revealed that its formula is  $\text{Fe}_2^{+3}\text{Al}_2\text{Si}_3\text{O}_{12}$  for almandine and  $\text{Mg}_3\text{Al}_2\text{Si}_3\text{O}_{12}$  for pyrope. With iron-oxygen bond  $\alpha$  and  $\gamma$ , iron adopts octahedral coordination geometry. It means that each Fe center is bound to six oxygen atoms. Magnesium oxide on the other hand, has a crystal structure [17] similar to that of sodium chloride. Fig.9 shows the crystal structure of magnesium oxide.

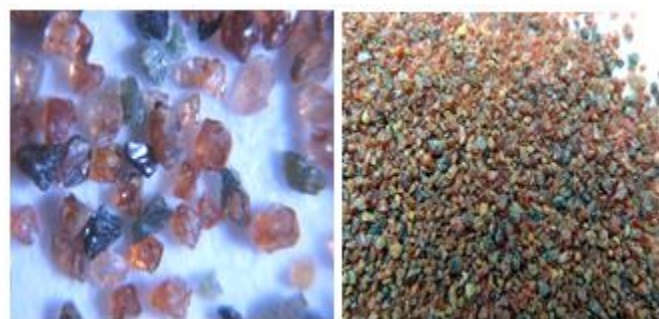
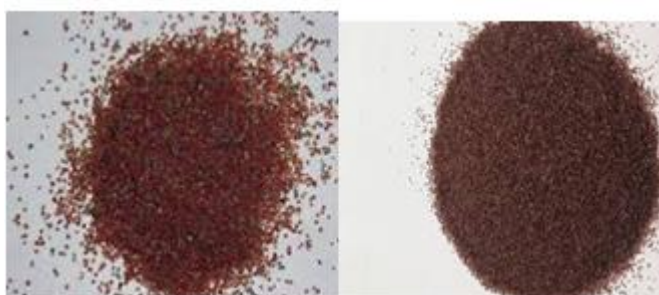


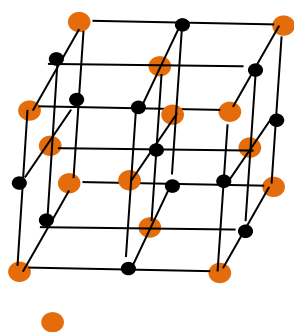
**Fig. 8a (x1000)**

**8b (x 80)**



**8c before heating**

**8d after heating**



compared to the same green mineral. The surface of the cut marble is more smooth and free of scratches..

## REFERENCES

**Fig. 9** the crystal structure of magnesium oxide

Both oxides of iron and magnesium form a solid solution with a strong bonding that cannot be deformed by thermal treatment. However, a crystal dislocation can take place by heating with subsequent oxidation of iron to a higher state of oxidation. Finite decrease in volume takes place and density value increases. As the density increases, the garnet material turns more compact and its abrasiveness increases. Heating at more than 600°C has deforms the compacted garnet particles and cause less hard and less abrasive material. It is therefore recommended that thermal treatment of raw garnet particles at 600°C max is in favor of improving the abrasiveness of the material. Fig.10a shows a piece of marble after cut with the garnet sample MF in the form of toothed disc. Fig.10b shows the smoothness of the cut surface.



**Fig. 10a** a toothed disc shaped with water cutting jet using MF garnet particles



**Fig. 10 b** the smoothness of the cut surface.

## IV. CONCLUSION

The output findings of this work is that heating clean almandine and pyrope garnet particles at 600°C for 5 h improves its hardness and abrasiveness properties. The workability of the heated garnet increases with 60 % as

- [1]. Yong-Nian Xu, Ching, W. Y. and Brickeen B. K.(2000) “Electronic structure and bonding in garnet crystals  $\text{Gd}_3\text{Sc}_2\text{Ga}_3\text{O}_{12}$ ,  $\text{Gd}_3\text{Sc}_2\text{Al}_3\text{O}_{12}$ , and  $\text{Gd}_3\text{Ga}_3\text{O}_{12}$  compared to  $\text{Y}_3\text{Al}_3\text{O}_{12}$  , Phys. Rev. B 2000, **61**, 181
  - [2]. Kuimari, K.K. Balaram V. and. Sirdeshmukh, L (1992), “Characterization and dielectric properties of Almandine-pyrope garnets” Bull. Mater. Sci. vol 15(3), 279-84
  - [3]. Mao et al., (2013), “Synchrotron Mössbauer study of Fe-bearing pyrope at high pressures and temperatures” American Mineralogist, Volume 98, pages 1146–1152, 2013
  - [4]. Huggins, F.E. (1975) The  $3d$  levels of ferrous ions in silicate garnets. American Mineralogist, 60, 316–319.
  - [5]. Amthauer. G., Annersten H. and Hafner S.S. (1976) The Mössbauer spectrum of Fe in silicate garnets. Zeitschrift für Kristallographie, 143, 14–55
  - [6]. Murad E. and Wagner F.E. (1987) The Mössbauer spectrum of almandine. Physics and Chemistry of Minerals, 14, 264–269
  - [7]. Geiger, C.A., Armbruster, T., Lager, G.A., Jiang, K., Lottermoser, W., and Amthauer, G. (1992) A combined temperature dependent Fe Mössbauer and single crystalX-ray diffraction study of synthetic almandine: Evidence for the Gol'danskii Karyagin Effect. Physics and Chemistry of Minerals, 19, 131–126.
  - [8]. Cerná. K., Mašlán ,M. and Martinec P. (2000) Mössbauer spectroscopy of garnets of almandine-pyrope series. Materials Structure, 7, 6–9.
  - [9]. Barcova, K. , Mashlan, M. Zboril, R. Martinec, P. Kula, P. (2000) Thermal decomposition of almandine garnet: Mössbauer study, Czechoslovak Journal of Physics, July 2001, Volume 51, [Issue 7](#), pp 749-754
  - [10]. Zboril, R. , Mashlan, M. Machala, L. Walla, J. Barcova, K. and Martinec P. (2004), Characterization and Thermal Behaviour of Garnets from Almandine–Pyrope Series at  $1200^\circ\text{C}$  Hyperfine Interactions 12-2004, Volume 156-157, [Issue 1-4](#), pp 403-410.
  - [11]. Zboril, R. , Mashlan, M. , Barcova, K. , Walla, J. Ferrow, E. and Martinec P. (2003) Thermal behaviour of pyrope at 1000 and  $1100^\circ\text{C}$ :

mechanism of  $\text{Fe}^{2+}$  oxidation and decomposition model Physics and Chemistry of Minerals November 2003, Volume 30, [Issue 10](#), pp 620-627

9	using MF garnet particles
10a	the smoothness of the cut surface.
10b	

[12]. Schneeweiss, O. , Zbořil, R. David, B. Heřmánek, M.and Mashlan M. (2009) Solid-state synthesis of  $\alpha$ -Fe and iron carbide nanoparticles by thermal treatment of amorphous  $\text{Fe}_2\text{O}_3$ , Proceedings of the International Symposium on the Industrial Applications of the Mössbauer Effect (ISIAME 2008) held in Budapest, Hungary, 17–22 August 2008 Editors: E. Kuzmann, K. Lázár

[13]. Abdel Aal<sup>1</sup>, A. Zaki, Z.I and Abdel Hamid Z. (2006) Novel composite coatings containing (TiC– $\text{Al}_2\text{O}_3$ ) powder, Materials Science and Engineering: A Vol. 447 (1–2), 25 February 2007, Pages 87–94

[14]. Mina, Nile Jet Imp & Exp :Co. Egypt  
 Email: [info@egyptmarblewaterjet.com](mailto:info@egyptmarblewaterjet.com)

[15]. NOVAK. G.A & GIBBS, G.V. (1971). Structure of sodium perbromate monohydrate - Crystallography Am. Mineral. 56, 791-825

[16]. Kimberly, E.K., Jonathan. F. , Stebbins<sup>1</sup>, I. , Lin-Shu T. Du<sup>1</sup>, Mosenfelder<sup>2</sup> , L. Paul. D. Asimow<sup>2</sup> and Charles, A, Geiger<sup>3</sup> (2008) Cation order/disorder behavior and crystal chemistry of pyrope-grossular garnets: An  $^{17}\text{O}$  3QMAS and  $^{27}\text{Al}$  MAS NMR spectroscopic study. American Mineralogist 93(1): 134-143 · January 2008

[17]. Krispin M. and Ullrich, A.(2012) Siegfried Hor Crystal structure of iron-oxide nanoparticles synthesized from ferritin,, Journal of Nanoparticle ResearchJanuary, 14:669

Figure Caption

Fig. #	Caption
1a, 1b	The cutting facility [14]
2	Effect of heating garnet mineral on the weight loss of the garnet particles
3	Effect of heating temperature on the particle size of garnet mineral
4	Effect of heating the MF garnet particles on bulk density value
5	Hardness in Mohs as a function of heat treatment of garnet MF particles
6	Effect of heating the garnet particles on the workability of the garnet particles.
7	The octahedral structure of garnet [15]
8	8a (x1000)                8b (x 80) 8c before heating            8d after heating the crystal structure of magnesium oxide toothed disc shape d with water cutting jet